Dynamic Susceptibility Contrast MRI at 7 T: Tail-Scaling Analysis and Inferences About Field Strength Dependence

Linda Knutsson[1,2], Xiang Xu[3,4], Freddy Ståhlberg[1,5,6], Peter B. Barker[3,4], Emelie Lind[1], Pia C. Sundgren[5], Peter C. M. van Zijl[3,4], and Ronnie Wirestam[1]

[1]Department of Medical Radiation Physics, Lund University, Lund, Sweden; [2]Department of Radiology (Adjunct), Johns Hopkins School of Medicine, Baltimore, Maryland; [3]Russell H. Morgan Department of Radiology and Radiological Science, Johns Hopkins University School of Medicine, Baltimore, Maryland; [4]F. M. Kirby Research Center for Functional Brain Imaging, Kennedy Krieger Institute, Baltimore, Maryland; [5]Department of Diagnostic Radiology, Lund University, Lund, Sweden; and [6]Lund University Bioimaging Center, Lund University, Lund, Sweden

Corresponding Author:
Linda Knutsson, PhD
Department of Medical Radiation Physics, Lund University,
Skane University Hospital, SE-221 85 Lund, Sweden;
E-mail: Linda.Knutsson@med.lu.se

ABSTRACT

Dynamic susceptibility contrast magnetic resonance imaging (DSC-MRI) following bolus injection of gadolinium contrast agent (CA) is widely used for the estimation of brain perfusion parameters such as cerebral blood volume (CBV), cerebral blood flow (CBF), and mean transit time (MTT) for both clinical and research purposes. Although it is predicted that DSC-MRI will have superior performance at high magnetic field strengths, to the best of our knowledge, there are no reports of 7 T DSC-MRI in the literature. It is plausible that the transfer of DSC-MRI to 7 T may be accompanied by increased R_2^* relaxivity in tissue and a larger difference in ΔR_2^*-versus-concentration relationships between tissue and large vessels. If not accounted for, this will subsequently result in apparent CBV and CBF estimates that are higher than those reported previously at lower field strengths. The aims of this study were therefore to assess the feasibility of 7 T DSC-MRI and to investigate the apparent field-strength dependence of CBV and CBF estimates. In total, 8 healthy volunteers were examined using DSC-MRI at 7 T. A reduced CA dose of 0.05 mmol/kg was administered to decrease susceptibility artifacts. CBV, CBF, and MTT maps were calculated using standard DSC-MRI tracer-kinetic theory. Subject-specific arterial partial volume correction factors were obtained using a tail-scaling approach. Compared with literature values obtained using the tail-scaling approach at 1.5 T and 3 T, the CBV and CBF values of the present study were found to be further overestimated. This observation is potentially related to an inferred field-strength dependence of transverse relaxivities, although issues related to the CA dose must also be considered.

INTRODUCTION

Dynamic susceptibility contrast magnetic resonance imaging (DSC-MRI) is used for the estimation of cerebral perfusion parameters such as cerebral blood volume (CBV), cerebral blood flow (CBF), and mean transit time (MTT) using the theory of intravascular tracers (1). Considering the ability of MRI to combine morphological and functional information during a single imaging session, this method can be used in both clinical and research environments. In the clinic, DSC-MRI is widely used for visualizing perfusion deficits in patients with vascular disease, particularly acute stroke, and for evaluating angiogenesis and blood volume in brain tumors.

High magnetic field strength (B_0) has a number of theoretical advantages for DSC-MRI; the larger magnetization can be used either to create images with higher signal-to-noise ratio or

higher spatial resolution, while the increased susceptibility effect (which scales linearly with field strength) increases contrast. The increased susceptibility effect can be used to reduce contrast agent (CA) dose or adjust imaging parameters (eg, shorter echo time [TE]) while maintaining similar contrast. However, when performing DSC-MRI at higher field strengths, susceptibility and chemical shift artifacts, B_1 inhomogeneity, and concerns about specific absorption rate are amplified. However, with appropriate sequence design, these problems can be overcome. The purpose of this study was to design a DSC-MRI protocol for 7 T that provides images with a visual appearance similar to those seen at lower field strengths. An additional aspect of this study was to investigate whether CBV and CBF estimates, in absolute terms, show any apparent field strength dependence when applying a conventional DSC-MRI quantification approach, that

is, assuming equal and concentration-independent R_2^* relaxivities in blood and tissue. Such an apparent CBV and CBF field-strength dependence would be related to previous predictions of an increased R_2^* relaxivity in tissue, accompanied by a larger difference in ΔR_2^*-versus-concentration relationships between tissue and large vessels, when moving from 1.5 T to 3 T (2). Hence, an additional aim of this study was to assess the apparent field-strength dependence of CBV and CBF by extracting quantitative perfusion estimates in healthy volunteers and comparing the 7 T estimates with corresponding literature values obtained at 1.5 T and 3 T.

In a typical DSC-MRI experiment, the limited spatial resolution implies that the arterial input function (AIF) data are likely to include signal components from the tissue surrounding the vessel (3). This may lead to distorted AIFs, and these partial volume effects (PVEs) often contribute to an overestimation of CBV and CBF when absolute quantification is performed. In addition, this source of overestimation may interfere with the field-strength-related overestimation effects to be evaluated in this study. Inclusion of a PVE-reduction approach in the analysis of the present data was therefore warranted (4-9). We used the PVE-reduction method referred to as "tail-scaling" (9), which uses the ratio of the steady-state concentration levels of the AIF and venous output function (VOF) as a scaling factor to correct for PVEs in the AIF.

In this study, the feasibility of DSC-MRI at 7 T was investigated in 8 healthy volunteers, and the apparent field-strength dependence of CBV and CBF after applying tail-scaling PVE correction was investigated through comparison with previously published literature values obtained by a similar methodology at 1.5 T and 3 T.

MATERIALS AND METHODS
Subjects and MR Imaging
In total 8 healthy volunteers (males, 5; age, 24–50 years) were examined using an actively shielded 7 T MRI scanner ('Achieva', Philips Healthcare LLC, Best, the Netherlands) and a 32-channel phased-array head coil (Nova Medical, Wilmington, MA). The project was approved by the local ethics committee (The Regional Ethical Review Board in Lund), and written informed consent was obtained from each volunteer. Morphological images (MPRAGE, before and after CA administration) of each volunteer were examined by an experienced neuroradiologist (PCS) to exclude any pathology.

A reduced dose (ie, half of the conventional dose) of gadoterate meglumine CA (0.05 mmol/kg body weight, Dotarem, Guerbet, Paris, France) was administered at an injection rate of 5 mL/s, and the DSC-MRI experiment was performed using single-shot gradient-echo echo-planar imaging with the following parameters: in-plane spatial resolution = 2×2 mm^2, section thickness = 3 mm, number of sections = 14–21, flip angle = 70°, repetition time = 1500 milliseconds, TE = 30 milliseconds, and SENSE acceleration factor = 2.0 with 120 dynamics. A 20-mL saline flush was injected at a rate of 5 mL/s after the CA administration. The parameters selected were similar to our clinical and research 3 T DSC-MRI protocol parameters, although with better resolution in the slice direction and with a slightly decreased in-plane resolution, giving us a voxel

volume of 12 mm^3 in our 7 T experiment compared with 15 mm^3 in our 3 T protocol. As part of an extended MRI protocol, an additional 0.1 mmol/kg CA dose, not used in this study, was injected ~9 minutes before the DSC-MRI CA injection.

Postprocessing
Concentrations C from the tissue and artery were obtained using the relationship $C(t) = -k \cdot (1/TE) \cdot \ln[S(t)/S_0]$, where $S(t)$ is the signal at time t, S_0 is the baseline (pre-CA) signal, and k is a constant reflecting the transverse relaxivity r2* when gradient-echo imaging is used. Because tissue and blood were presumed to have equal and concentration-independent relaxivities, k was set to 1. The arterial concentration time course, that is, the arterial input function, is denoted as AIF(t) below.

CBF and CBV without any correction were calculated using the standard DSC-MRI theory based on the central volume theorem and Zierler's area-to-height relationship (10-12):

$$CBV = \frac{(1 - H_{\text{large}}) \int\limits_0^\infty C_t(t)\,dt}{\rho(1 - H_{\text{small}}) \int\limits_0^\infty AIF(t)\,dt} \qquad (1)$$

$$CBF = \frac{(1 - H_{\text{large}}) R_{\max} \int\limits_0^\infty C_t(t)\,dt}{\rho(1 - H_{\text{small}}) \int\limits_0^\infty R(t)\,dt \int\limits_0^\infty AIF(t)\,dt} \qquad (2)$$

H_{large} and H_{small} are the hematocrit values in large and small vessels, respectively; ρ is the mean whole-brain tissue density; and the factor $(1 - H_{\text{large}})/[\rho\,(1 - H_{\text{small}})]$ was set to 0.705 cm^3/g (12). The measured tissue concentration–time curve $C_t(t)$ was deconvolved with the AIF to obtain the tissue impulse response function R(t) (and its peak value $R_{\max}$). A block-circulant singular value decomposition algorithm (13), with a fixed cutoff value of 10%, was used for the deconvolution. A global AIF was obtained by locating 4–8 arterial pixels in the middle cerebral artery branches in the Sylvian fissure region and averaging the corresponding concentration curves. The individual arterial curves were required to show nondistorted peaks with an early rise and high maximum concentration (14). MTT was calculated using the central volume theorem, that is, MTT = CBV/CBF.

Tail Scaling
The VOF was obtained by taking the mean value of concentration–time curves corresponding to ~3 pixels within the sagittal sinus (from 2 to 3 different slices). Geometric distortions and/or signal saturation in the venous first-passage bolus peak were interpreted as signs of a high fraction of vascular signal, so VOFs based on venous curves with distorted first-passage shape were favored for calibration, because these voxels are likely to show less PVEs than undistorted venous concentration–time curves. Another issue to take into account is that VOFs showing a signal pixel shift that is visible throughout the steady-state phase should be avoided, because such an effect implies that the steady-state signal in a given image pixel originates from a

different tissue location compared with the pre-CA baseline, which affects the concentration calculation. Hence, the criteria for selecting sagittal sinus VOFs in this study were that the individual concentration curves should display distortions (eg, flat or double-peak) during the first passage of the CA bolus, as this implies high CA content in the voxel and thereby minimal PVEs, and show either a minimal or absent pixel shift throughout the steady-state phase (15).

Subject-specific correction factors using the tail-scaling approach were obtained by calculating the mean concentration level of data points registered at the steady-state phase (40 time points) of the AIF and by dividing this mean value by the mean concentration level of the data points registered at the steady-state phase of the VOF (40 time points). No part of the recirculation phase was included in these data points.

For the perfusion evaluation, gray matter (GM) CBV and CBF estimates from the tail-scaling approach were extracted from manually selected regions of interest (ROIs) in the thalamus. In a similar fashion, frontal white matter (WM) estimates were also retrieved using manually applied ROIs. The correction factors from tail scaling were thereafter applied to the CBV and CBF GM and WM ROI mean values to correct the estimates for PVEs.

RESULTS

A mean GM CBF estimate of (114 ± 20) mL/min/100 g and a mean GM CBV estimate of (12.6 ± 2.8) mL/100 g were obtained (n = 8). For WM, the estimated mean CBF value was (47.3 ± 9.9) mL/min/100 g and the CBV estimate was (6.3 ± 1.0) mL/100 g. The GM-to-WM ratios were 2.4 for CBF and 2.0 for CBV. The mean MTT estimates for GM and WM were 6.6 and 8.0, respectively. Note that no pronounced field-strength dependence is expected in the MTT calculation because relaxivity changes are divided out when using the central volume theorem.

With regard to image quality, Figure 1A shows representative 7 T CBF, CBV and MTT maps from one volunteer, with similar visual appearance as the DSC-MRI maps normally obtained at lower field strengths. Note that no obvious distortions are seen in the images despite being acquired at 7 T. In addition, the CBV and CBF contrast between GM and WM is clearly visible. For comparison of image quality, a 3 T DSC-MRI data set from Knutsson et al.'s study (15) is also displayed (Figure 1B).

Figure 2 shows an example of AIF and VOF concentration–time curves in one subject. The VOF concentration–time curve shows peak distortions and a noisier steady-state concentration phase. Note that the last 40 time points were used for the tail-scaling PVE correction

DISCUSSION

To the best of our knowledge, this is the first report showing that DSC-MRI is feasible at 7 T. Although numerous challenges occur when moving from 3 T to 7 T MRI, these issues can, as shown in this study, largely be remediated by appropriate protocol designs. The question whether there is any advantage of using an ultrahigh field system for clinical perfusion research is also relevant in this context, and a reasonable answer would be to point out that one only needs half the normal amount of the CA, which may reduce the costs and also the potential risks associ-
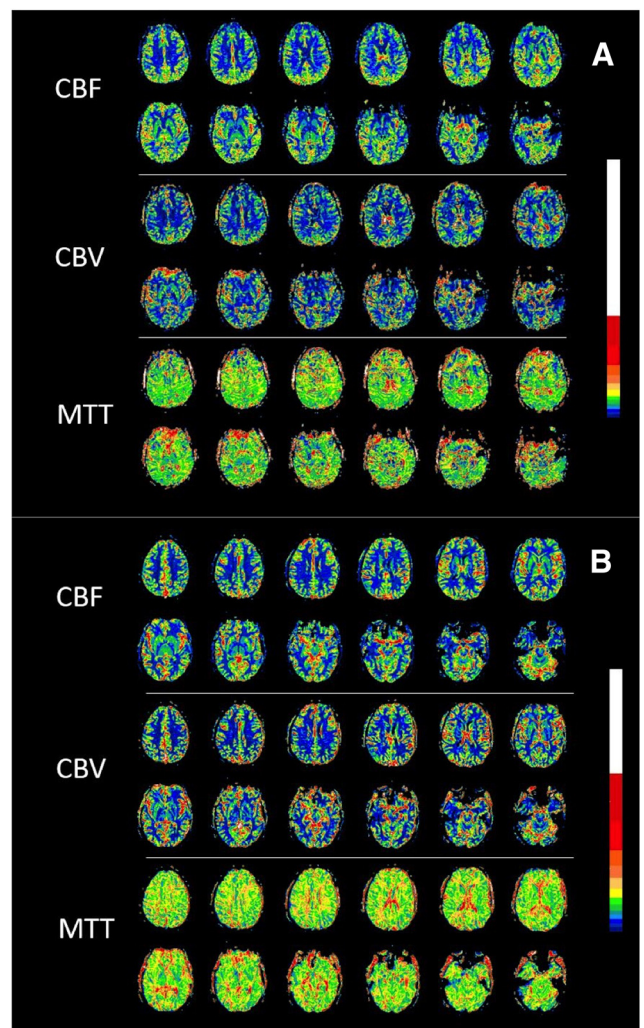
Figure 1. Dynamic susceptibility contrast magnetic resonance imaging (DSC-MRI) cerebral blood flow (CBF) (top), cerebral blood volume (CBV) (middle), and mean transit time (MTT) (bottom) maps from healthy volunteers obtained at 7 T (12 out of 14 sections are shown) (A) and 3 T (12 out of 20 sections shown) (B). The 3 T imaging parameters are given in Knutsson et al.'s study (15). To facilitate visual comparison, the parametric maps in (A) and (B) are displayed as relative values. Red indicates high values and blue indicates low values. Note that the visual appearance is similar to what can be expected at lower field strengths, although the 7 T acquisition allowed for a significant contrast agent (CA) dose reduction.

ated with nephrogenic systemic fibrosis and the effects of long-term tissue accumulation after repeated use of gadolinium, as recently reported by the Food and Drug Administration (16).

The primary finding of this study was the elevated CBV and CBF estimates compared with those given in prior literature values at 1.5 T and 3 T, which may be related to differences in
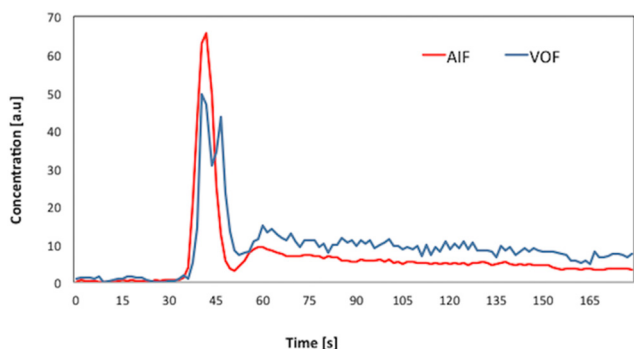
Figure 2. Example of arterial input function (AIF) and venous output function (VOF) concentration–time curves. The last 40 time points (last 60 seconds, from 120 to 180 seconds) of each curve were used to calculate the mean steady-state concentration level.

Table 1. Gray and white matter CBF and CBV estimates obtained using the tail-scaling approach at different field strengths

	1.5 T (Ref. 9)	3 T (Ref. 15)	7 T (this study)
CBF GM [mL/min/100 g]	58	80	114
CBF WM [mL/min/100 g]	30		47.3
CBV GM [mL/100 g]	4.57		12.6
CBV WM [mL/100 g]	2.3		6.3

tissue and blood R_2^* relaxivity as a function of field strength. In the present study, mean absolute CBF estimates of 114 mL/min/100 g in GM and 47.3 mL/min/100 g in WM were obtained, whereas mean absolute CBV estimates were 12.6 mL/100 g in GM and 6.3 mL/100 g in WM. These estimates should be compared with data from previous studies using tail scaling (Table 1). In healthy volunteers, Knutsson et al. observed an absolute CBF value of 80 mL/min/100 g in GM (CBV and WM data not available) (15). Bjørnerud et al. (9) applied tail scaling to patient DSC-MRI data obtained at 1.5 T and observed CBF values of 58 mL/min/100 g in GM and 30 mL/min/100 g in WM, whereas the CBV values were 4.57 mL/100 g in GM and 2.3 mL/100 g in WM.

There are differences and similarities between these 3 studies. The study at 1.5 T included 101 patients, and the experiments were conducted using a CA dose of 0.2 mmol/kg with a spatial voxel volume of 16 mm³. Furthermore, the VOF was selected using automated cluster analysis, and, similar to the present approach, the steady-state phase of the concentration–time curve was used together with the same tracer-kinetic model and deconvolution method. However, a difference between the present study and the 1.5 T study was that Bjørnerud et al. made a gamma-variate fitting to the measured concentration and time. The 3 T study included 20 healthy volunteers and the VOF was selected manually, as in the present study, but the tail-scaling data points, for both AIFs and VOFs, also included the recirculation peak. In addition, the CA dose was 0.1 mmol/kg in the 3 T study, and the spatial resolution was slightly lower than that in the present study.

The 7 T GM-to-WM CBF and CBV ratios of the present study were 2.4 and 2.0, respectively, compared with those of the 1.5 T study (9), which showed ratios of 1.9 and 2.0, respectively. In a study by Wirestam et al. (17), at 1.5 T, the GM-to-WM CBF ratio was 2.2 using standard singular value decomposition. The comprehensive PET study by Leenders et al. (18) showed GM-to-WM ratios of 2.5 for CBF and 1.9 for CBV, which are in good

agreement with the present study. From these results, no conclusions can be drawn regarding any field-strength dependence of *relative* DSC-MRI values in different tissue types.

With regard to the absolute CBV and CBF estimates, the present study results and those of the comparisons with previous studies are not entirely straightforward to interpret because CA dose, TE, and spatial resolution differed between the 1.5 T (9), 3 T (15) and 7 T investigations. Kjølby et al. (2) used simulations to calculate an r2* value of 44 mM⁻¹s⁻¹ at 1.5 T and 87 mM⁻¹s⁻¹ at 3 T, that is, indicating a substantial linear field-strength dependence of the tissue relaxivity. Wirestam et al. (19) estimated the in vivo R_2^* relaxivity at 3 T to be ~32 mM⁻¹s⁻¹, based on a comparison with a reference arterial spin labeling CBF method. In two studies investigating oxygenated whole-blood relaxivity (20, 21), a nonlinear relationship was observed between the concentration C and ΔR_2^*, contrary to the linear ΔR_2^*-versus-C relationship found typically in tissue. One plausible cause of CBV and CBF overestimations is that relaxivities of blood and tissue differ (otherwise k, defined above, would be the same for blood and tissue and cancel out in the kinetic equations), and a CBV and CBF field-strength dependence requires that this difference changes with increased B_0. When CA is added to the plasma volume, the susceptibility differences between the plasma compartment and its surroundings will change, leading to altered local gradients and thereby altered R_2^*. The topography of the capillary–tissue interface differs substantially from the plasma–red blood cells interface in whole blood, and the R_2^* relaxivity of CA residing in intravascular plasma is thus dependent on the local environment, and it has been shown to be higher in tissue compartments than in whole blood (2). At higher field strengths, the susceptibility effects increase proportionally, and the change in R_2^* at a given CA concentration will be more prominent (ie, the R_2^* relaxivity is increased), and the increased susceptibility effects also imply that the difference in CA-induced ΔR_2^* between tissue and blood is enhanced at a higher field strength (2), which may explain our elevated estimates compared with literature values obtained at lower field strengths.

Furthermore, in whole blood, the susceptibility difference between red blood cells and plasma varies with CA concentration in a rather complex manner (22), leading to a nonlinear ΔR_2^*-versus-C relationship, implying that absolute estimates according to equations (1)–(2) also depend on CA dose. In theory, the blood-versus-tissue differences in CA response are reduced at higher dose because of the nonlinear ΔR_2^*-versus-C relationship in blood (2), and the low dose used at the 7 T would thus

increase this difference. However, it is not evident that the registered AIF signal originates from whole blood only, and in such a case, the exact shape of the $\Delta R2^*$-versus-C relationship is unknown.

A drawback of this quantification approach at ultrahigh field strength is that venous steady-state pixel shifts are more pronounced in 7 T images, making it more difficult for the user to find suitable VOFs. An approach that would facilitate VOF registration would be to use a prebolus injection with a low dose, as in the study by Knutsson et al. ([8]). Alternatively, a sufficiently high bandwidth would remove the pixel shifts, but it would be difficult to achieve total volume coverage with reasonable temporal resolution ($\sim$1.5 seconds) with high-bandwidth readout techniques. The problem of competing T1 effects ([1]) may also

pose a problem because of the longer T1 in blood at 7 T, resulting in AIF and VOF underestimations.

In conclusion, a well-designed protocol can reduce susceptibility artifacts at ultrahigh field strength, and perfusion maps of clinically useful quality, at reduced CA dose, can be obtained. The study further indicated that an apparent field-strength dependence of absolute CBV and CBF estimates may be found, potentially related to an increased tissue R_2^* relaxivity accompanied by a larger blood-versus-tissue difference in ΔR_2^*-versus-concentration relationships at higher field strengths. Obviously, true CBV and CBF are not field strength-dependent and this means that the theory for quantifying CBV and CBF from DSC-MRI experiments remains incomplete.

REFERENCES

1. Knutsson L, Ståhlberg F, Wirestam R. Absolute quantification of perfusion using dynamic susceptibility contrast MRI: pitfalls and possibilities. Magn Reson Mater Phys. 2010;23(1):1–21.
2. Kjølby BF, Østergaard L, Kiselev VG. Theoretical model of intravascular paramagnetic tracers effect on tissue relaxation. Magn Reson Med. 2006;56(1):187–197.
3. van Osch MJ, Vonken EJ, Bakker CJ, Viergever MA. Correcting partial volume artifacts of the arterial input function in quantitative cerebral perfusion MRI. Magn Reson Med. 2001;45(3):477–485.
4. Kellner E, Mader I, Mix M, Splitthoff DN, Reisert M, Foerster K, Nguyen-Thanh T, Gall P, Kiselev VG. Arterial input function measurements for bolus tracking perfusion imaging in the brain. Magn Reson Med. 2013;69(3):771–780.
5. Knutsson L, Börjesson S, Larsson E-M, Risberg J, Gustafson L, Passant U, Ståhlberg F, Wirestam R. Absolute quantification of cerebral blood flow in normal volunteers: Correlation between Xe-133 SPECT and dynamic susceptibility contrast MRI. J Magn Reson Imaging. 2007;26(4):913–920.
6. Zaharchuk G, Bammer R, Straka M, Newbould RD, Rosenberg J, Olivot JM, Mlynash M, Lansberg MG, Schwartz NE, Marks MM, Albers GW, Moseley ME. Improving dynamic susceptibility contrast MRI measurement of quantitative cerebral blood flow using corrections for partial volume and nonlinear contrast relaxivity: A xenon computed tomographic comparative study. J Magn Reson Imaging. 2009;30(4):743–752.
7. Crane DE, Donahue MJ, Chappell MA, Sideso E, Handa A, Kennedy J, Jezzard P, MacIntosh BJ. Evaluating quantitative approaches to dynamic susceptibility contrast MRI among carotid endarterectomy patients. J Magn Reson Imaging. 2013; 37(4):936–943.
8. Knutsson L, Lindgren E, Ahlgren A, van Osch MJ, Bloch KM, Surova Y, Ståhlberg F, van Westen D, Wirestam R. Dynamic susceptibility contrast MRI with a prebolus contrast agent administration design for improved absolute quantification of perfusion. Magn Reson Med. 2014;72(4):996–1006.
9. Bjørnerud A, Emblem KE. A fully automated method for quantitative cerebral hemodynamic analysis using DSC-MRI. J Cereb Blood Flow Metab. 2010;30(5): 1066–1078.
10. Meier P, Zierler KL. On the theory of the indicator-dilution method for measurement of blood flow and volume. J Appl Physiol. 1954;6(12):731–744.
11. Zierler KL. Equations for measuring blood flow by external monitoring of radioisotopes. Circ Res. 1965;16:309–321.
12. Rempp KA, Brix G, Wenz F, Becker CR, Gückel F, Lorenz WJ. Quantification of regional cerebral blood flow and volume with dynamic susceptibility contrast-enhanced MR imaging. Radiology. 1994;193(3):637–641.

13. Wu O, Østergaard L, Weisskoff RM, Benner T, Rosen BR, Sorensen AG. Tracer arrival timing-insensitive technique for estimating flow in MR perfusion-weighted imaging using singular value decomposition with a block-circulant deconvolution matrix. Magn Reson Med. 2003;50(1):164–174.
14. Thilmann O. LUPE: An extensible modular framework for evaluation of DSC-acquired perfusion images. Magn Reson Mater Phys. 2004;16(electronic suppl. 1):537.
15. Knutsson L, Lindgren E, Ahlgren A, van Osch MJ, Markenroth Bloch K, Surova Y, Ståhlberg F, van Westen D, Wirestam R. Reduction of arterial partial volume effects for improved absolute quantification of DSC-MRI perfusion estimates: comparison between tail scaling and prebolus administration. J Magn Reson Imaging. 2015;41(4):903–908.
16. McDonald RJ, McDonald JS, Kallmes DF, Jentoft ME, Murray DL, Thielen KR, Williamson EE, Eckel LJ. Intracranial gadolinium deposition after contrast-enhanced MR imaging. Radiology. 2015;275(3):772–782.
17. Wirestam R, Andersson L, Ostergaard L, Bolling M, Aunola JP, Lindgren A, Geijer B, Holtås S, Ståhlberg F. Assessment of regional cerebral blood flow by dynamic susceptibility contrast MRI using different deconvolution techniques. Magn Reson Med. 2000;43(5):691–700.
18. Leenders KL, Perani D, Lammertsma AA, Heather JD, Buckingham P, Healy MJR, Gibbs JM, Wise RJS, Hatazawa J, Herold S, Beaney RP, Brooks DJ, Spinks T, Rhodes C, Frackowiak RSJ, Jones T. Cerebral blood flow, blood volume and oxygen utilization. Normal values and effect of age. Brain. 1990;113 (Pt 1):27–47.
19. Wirestam R, Lind E, Ahlgren A, Ståhlberg F, Knutsson L. Dynamic susceptibility contrast perfusion MRI using phase-based venous output functions: comparison with pseudo-continuous arterial spin labelling and assessment of contrast agent concentration in large veins. Magn Reson Mater Phys. 2016;29(6):823–831.
20. van Osch MJ, Vonken EJ, Viergever MA, van der Grond J, Bakker CJ. Measuring the arterial input function with gradient echo sequences. Magn Reson Med. 2003;49(6):1067–1076.
21. Akbudak E, Kotys M, Conturo T. Quadraticity and hematocrit dependence of $\Delta R2^*$ AIF signals at 3T: a blood phantom study under physiologic conditions. Syllabus of the ISMRM workshop on Quantitative Cerebral Perfusion Imaging Using MRI: A technical perspective, Venice, 2004:10–11.
22. Blockley NP, Jiang L, Gardener AG, Ludman CN, Francis ST, Gowland PA. Field strength dependence of R1 and R2* relaxivities of human whole blood to ProHance, Vasovist, and deoxyhemoglobin. Magn Reson Med. 2008;60(6):1313–1320.